Theoretical model for diffusion-reaction based drug delivery from a multilayer spherical capsule

Ankur Jain [a,*], Sean McGinty [b,c], Giuseppe Pontrelli [d], Long Zhou [e]

[a] Mechanical and Aerospace Engineering Department, University of Texas at Arlington, Arlington, TX, USA
[b] Division of Biomedical Engineering, University of Glasgow, Glasgow, UK
[c] Glasgow Computational Engineering Centre, University of Glasgow, Glasgow, UK
[d] Istituto per le Applicazioni del Calcolo – CNR Via dei Taurini 19, Rome 00185, Italy
[e] School of Mechanical and Power Engineering, Henan Polytechnic University, Jiaozuo, Henan, China

ARTICLE INFO

ABSTRACT

Controlled drug delivery from a multilayer spherical capsule is used for several therapeutic applications. Developing a theoretical understanding of mass transfer in the multilayer capsule is critical for understanding and optimizing targeted drug delivery. This paper presents an analytical solution for the mass transport problem in a general multilayer sphere involving diffusion as well as drug immobilization in various layers due to binding reactions. An eigenvalue-based solution for this multilayer diffusion-reaction problem is derived in terms of various non-dimensional quantities including Sherwood and Damköhler numbers. It is shown that unlike diffusion-reaction problems in heat transfer, the present problem does not admit imaginary eigenvalues. The effect of binding reactions represented by the Damköhler numbers and outer surface boundary condition represented by the Sherwood number on drug delivery profile is analyzed. It is shown that a low Sherwood number not only increases drug delivery time, but also reduces the total mass of drug delivered. The mass of drug delivered is also shown to reduce with increasing Damköhler number. The impact of shell thickness is analyzed. The effect of a thin outer coating is accounted for by lumping the mass transfer resistance in series with convective boundary resistance, and a non-dimensional number involving the thickness and diffusion coefficient of the coating is shown to govern its impact on drug delivery characteristics. The analytical model presented here improves the understanding of mass transfer in a multilayer spherical capsule in presence of binding reactions, and may help design appropriate experiments for down-selecting candidate materials and geometries for drug delivery applications of interest.

© 2021 Elsevier Ltd. All rights reserved.

1. Introduction

Targeted release of a drug from an appropriately designed capsule is of much interest in a variety of therapeutics [1]. Compared to traditional mechanisms of drug delivery, targeted release from a capsule offers enhanced efficacy, reduced side effects and the possibility of personalized medicine [2,3]. The capsule usually comprises a drug-loaded core surrounded by one or more encapsulant layers that provide mechanical stability, chemical protection from the ambient, and may also be used for controlling the rate of release of the drug. A thin coating on the outer surface is also often provided for similar reasons [4,5].

It is important to understand the factors that govern the rate of drug delivery into the release medium. Experimental investigation of targeted drug delivery, especially *in vivo*, is expensive and cumbersome. Therefore, theoretical modeling of targeted drug release may play a critical role in down selecting candidate designs and materials, and in guiding the design of effective experiments. A comprehensive understanding of the processes that affect drug delivery may help design next-generation drug delivery systems, towards personalized medicine [2,3].

Depending on the physicochemical properties of the drug-loaded capsule, several different mechanisms may govern the release rate of the drug. It is usually assumed that diffusion is the key process, with the radial concentration gradient driving the drug release [6]. However, if the drug is loaded in a solid form, it may first need to undergo a dissolution process before being made available for diffusion [7]. The rate at which the drug dissolves

* Corresponding author at: 500W First St, Rm 211, Arlington, TX, USA 76019.
E-mail address: jaina@uta.edu (A. Jain).

Nomenclature

c	concentration (mol m^{-3})
D	diffusion coefficient (m^{2}s^{-1})
$\overline{D}$	non-dimensional diffusion coefficient
h	mass transfer coefficient (ms^{-1})
i	unit imaginary number, $i = \sqrt{-1}$
M	number of layers
N	non-dimensional eigenfunction norm
R	radius (m)
r	radial coordinate (m)
Sh	Sherwood number
t	time (s)
β	reaction rate (s^{-1})
$\overline{\beta}$	non-dimensional reaction rate
γ	non-dimensional interface location
τ	non-dimensional time
$\overline{\psi}$	cumulative fraction of drug released
$\overline{\chi}$	cumulative fraction of drug absorbed in each layer
$\overline{\rho}$	fraction of drug remaining in each layer
θ	non-dimensional concentration
ξ	non-dimensional radial coordinate
λ	non-dimensional eigenvalue
σ	drug partition coefficient

Subscripts

m	layer number
ref	reference value
in	initial value

is highly dependent on the properties of the drug and release medium, for example solubility, temperature and pH, among other factors. However, in many cases, the drug is either readily available in a dissolved form, or dissolves on a much faster timescale than that of diffusion. In such cases, the dissolution process can reasonably be neglected. As the drug diffuses outwards, some of it may irreversibly bind to components of the core and/or shell, resulting in reduction in mass of drug delivered. Such binding may be a pH-dependent process and has previously been approximated by first-order reaction kinetics [8]. On the outer surface of the core-shell composite, the drug is released into the medium with a mass flux that depends on the convective boundary conditions on the outer surface. In some cases, for example, when the capsule is suspended in a large volume of biofluid, the outer boundary condition may be modeled as an infinite sink, i.e. a zero concentration condition. In other cases, for example, when the outside medium is a tissue, a general convective boundary condition may be more appropriate. Key parameters that govern the overall drug release rate over time include diffusion coefficients in the core and shell, reaction rates associated with binding reactions, parameters governing transport at the core-shell interface and the convective mass transfer coefficient on the outer boundary. Comprehensive theoretical analysis of the drug diffusion and delivery process is critically needed to understand the role of these parameters and optimize system performance.

From a mass transfer perspective, the problem of drug delivery from a multilayer capsule may be interpreted as a diffusion-reaction problem [1]. In the present case, a balance between drug diffusion across layers, binding reactions in each layer and convective conditions on the outer surface determines the dynamics of drug concentration distribution within the capsule and the rate of drug delivered over time. Diffusion-reaction problems have been investigated for a variety of applications, including Li-ion batteries [9], biofilm growth [10], plasma systems [11], reactor design

[12] and biology [13]. In the field of drug delivery, the simplest models are either empirical with no physical description of the underlying drug release mechanism, or based upon the assumption that diffusion alone governs the drug release. Past papers and textbooks offer details on such models [14,15,16]. Notwithstanding, more comprehensive mechanistic models have been developed in the context of drug delivery, incorporating linear and non-linear, irreversible and reversible, saturable and non-saturable binding kinetics, as well as descriptions of other physical processes such as degradation, erosion, swelling, and osmotic pumping [17,18,19]. These models almost always require numerical solution due to their complexity. Often, however, modeling all of these processes is unnecessary, since the slowest process ultimately determines the release rate.

While diffusion-reaction systems have been studied in detail for a variety of applications, there is a relative lack of studies on diffusion-reaction in a multilayer body, as is relevant for the present work. A recent paper presented analysis of diffusion-reaction in a multilayer Li-ion cell [9]. Some work also exists in the context of drug diffusion in a two-layer or three-layer structure [20–24], but these studies are focused on specific problems, do not present generalized multilayer analysis and often rely on numerical analysis. On the other hand, analytical solutions may be desirable compared to numerical solutions because of the fundamental insights that analytical solutions provide, as well as the potential improvement in computational cost and complexity.

Analytical solutions for pure-diffusion multilayer problems using the separation of variables technique are well-known [25, 26]. These analytical solutions express the temperature/concentration in a series solution and utilize the boundary and interface conditions to determine the eigenvalues. However, such standard solutions do not readily apply to multilayer diffusion-reaction problems. Extension to a general *M*-layer spherical diffusion-reaction problem of interest here is not straightforward, since the reaction term may introduce additional complications in the analytical technique.

A key aspect of theoretical and practical interest in eigenfunction-based series solution of multilayer diffusion-reaction problems is the occurrence of imaginary eigenvalues. As shown recently, imaginary eigenvalues lead to a runaway situation in the system, and may arise when reaction-driven generation dominates over diffusion and removal from the boundaries [9]. While this has been studied in the context of heat transfer in Li-ion cells [9], a similar diffusion-reaction mass transfer analysis in a multilayer capsule may be of much interest. Note that unlike previously studied heat transfer problems, where heat may be either generated or absorbed due to reaction, in the present problem, only drug absorption driven by binding reactions is relevant.

This paper presents theoretical analysis of drug delivery from a multilayer spherical capsule. The analysis accounts for diffusion and reaction in a multi-layer spherical body and includes a general mass transfer boundary condition on the outer surface. The analysis predicts the drug release profile over time, and its dependence on various problem parameters including geometry, diffusion coefficients, reaction constants and conditions on the outer surface. It is shown that within the parameter space of relevance to common drug systems of interest, the reaction constants, along with the convective boundary condition on the outer surface, play a key role in determining the mass of drug delivered, as well as the time constant of the drug delivery process. The analytical solution presented here accounts for key aspects of drug delivery dynamics and provides useful insights into the drug delivery process. Through the relationships between various non-dimensional parameters, it can be used to identify simple relationships or clinical indicators of biomechanical significance.
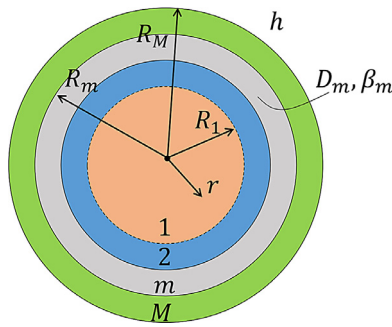
Fig. 1. Schematic of the geometry of the M-layer spherical diffusion-reaction problem.

2. Problem definition and derivation of solution

2.1. Problem definition

Fig. 1 shows a schematic of the problem of interest here. Consider the problem of drug release from a spherical capsule, made of M concentric layers of inner and outer radii R_{m-1} and R_m, respectively, and constant diffusion coefficients D_m ($m = 1,2....,M$). The inner-most layer is a spherical core of radius R_1. While the most common case is that of initial drug loaded only in the core ($m = 1$), a general assumption of the drug being initially loaded in one or more layers is made. The capsule is assumed to erode over a timescale much larger than the timescale for drug delivery, so that the geometry may be assumed to remain invariant for the present analysis. As time passes, the drug diffuses through the various layers and eventually releases into the environment at the outer surface of the sphere. In addition to diffusion, a chemical reaction occurring in the layers results in absorption of some of the drug within the sphere. Such a reaction is undesirable as it traps the drug within the capsule and reduces the mass of drug released into the external medium. In the absence of experimental evidence, this reaction is assumed to be first-order, i.e., with a constant rate β_m. Drug release at the outer surface is assumed to be governed by a general mass transfer boundary condition with coefficient h. A limiting case of this boundary condition would be $h \rightarrow \infty$, corresponding to zero concentration at the boundary, i.e., the surrounding medium acts as an infinite sink. The initial concentration in the mth layer is taken to be $c_{m,in}(r)$. While most drug-delivery capsules are designed to be two-layer, i.e., a core surrounded by a shell, a general M-layer analysis is presented here first, followed by derivation of the results for the special case of a two-layer system.

The problem is assumed to be axisymmetric, so that the concentration field is a function only of r and t. Assuming that all of the drug is initially dissolved (or dissolves at a timescale much faster than the diffusion timescale) and available for diffusion, the governing conservation equation for c_m, the concentration in the mth layer may be written as:

$$\frac{\partial c_m}{\partial t} = D_m \frac{1}{r^2} \frac{\partial}{\partial r}\left(r^2 \frac{\partial c_m}{\partial r}\right) - \beta_m c_m \quad R_{m-1} < r < R_m \ (m = 1, 2, 3 \ldots M) \tag{1}$$

which represents a balance between diffusion, reaction and transient terms.

The associated boundary conditions are

$$c_1 \text{ is finite} \quad \text{as } r \rightarrow 0 \tag{2}$$

$$-D_M \frac{\partial c_M}{\partial r} = h c_M \quad \text{at } r = R_M \tag{3}$$

At the interfaces, the following conditions apply

$$c_{m+1} = \sigma_m c_m \text{ at } r = R_m \ (m = 1, 2 \ldots M - 1) \tag{4}$$

$$D_m \frac{\partial c_m}{\partial r} = D_{m+1} \frac{\partial c_{m+1}}{\partial r} \text{ at } r = R_m \ (m = 1, 2 \ldots M - 1) \tag{5}$$

where σ_m is the drug partition coefficient [27], assumed to the independent of the concentration field [28]. In general, σ_m may depend on the concentration field in nonlinear reaction-diffusion systems, where saturable binding occurs on a timescale much quicker than diffusion [29], however, this is clearly not the case here, and assuming a constant partition coefficient is reasonable. Note that σ_m is a measure of how much the drug prefers to be in one layer compared with the next, and depends on various factors including the lipophilicity of the drug. When the layer materials are similar in terms of interactions with the drug, $\sigma_m = 1$, indicating continuity of concentration.

The initial condition is given by

$$c_m = c_{m,in}(r) \quad \text{at } t = 0 \ (m = 1, 2, 3 \ldots M) \tag{6}$$

2.2. Nondimensionalization

In order to non-dimensionalize the problem, the following variables are introduced:

$$\theta_m = \frac{c_m}{c_{ref}}, \xi = \frac{r}{R_M}, \tau = \frac{D_M t}{R_M^2}, \gamma_m = \frac{R_m}{R_M}, \bar{D}_m = \frac{D_m}{D_M},$$

$$\bar{\beta}_m = \frac{\beta_m R_M^2}{D_M}; \theta_{m,in} = \frac{c_{m,in}}{c_{ref}}, Sh = \frac{h \cdot R_M}{D_M}.$$

Here, c_{ref} is a reference concentration, which may be chosen as the maximum concentration at the initial time, which is usually the concentration in the core. Note that $\bar{\beta}_m$ is the Damköhler number for the mth layer that represents the reaction process, and Sh is the Sherwood number that represents mass transfer at the boundary.

Based on this, the governing equations may be re-written in non-dimensional form as follows:

$$\frac{\partial \theta_m}{\partial \tau} = \frac{\bar{D}_m}{\xi^2} \frac{\partial}{\partial \xi}\left(\xi^2 \frac{\partial \theta_m}{\partial \xi}\right) - \bar{\beta}_m \theta_m \quad \gamma_{m-1} < \xi < \gamma_m (m = 1, 2, 3 \ldots M) \tag{7}$$

subject to

$$\theta_1 \text{ is finite} \quad \text{as } \xi \rightarrow 0 \tag{8}$$

$$\frac{\partial \theta_M}{\partial \xi} + Sh \cdot \theta_M = 0 \quad \text{at } \xi = 1 \tag{9}$$

$$\theta_{m+1} = \sigma_m \theta_m \quad \text{at } \xi = \gamma_m (m = 1, 2 \ldots M - 1) \tag{10}$$

$$\bar{D}_m \frac{\partial \theta_m}{\partial \xi} = \bar{D}_{m+1} \frac{\partial \theta_{m+1}}{\partial \xi} \quad \text{at } \xi = \gamma_m (m = 1, 2 \ldots M - 1) \tag{11}$$

along with the following initial condition:

$$\theta_m = \theta_{m,in}(\xi) \quad \text{at } \tau = 0 \ (m = 1, 2, ..M) \tag{12}$$

Eqs. (7)-(12) define the spherical multilayer diffusion-reaction problem in non-dimensional form.

2.3. Solution methodology

A solution for Eqs. (7)-(12) may be obtained using the separation of variables technique in the following series form:

$$\theta_m(\xi, \tau) = \sum_{n=1}^{\infty} g_n f_{m,n}(\xi) \exp\left(-\lambda_n^2 \tau\right) \tag{13}$$

where g_n is a coefficient. By separating out the spatial and time-dependent terms, it can be shown that

$$f_{m,n}(\xi) = A_{m,n} \frac{\cos(\omega_{m,n}\xi)}{\xi} + B_{m,n} \frac{\sin(\omega_{m,n}\xi)}{\xi} \tag{14}$$

where, by inserting Eqs. (13) and (14) in Eq. (7), it can be shown that

$$\omega_{m,n} = \sqrt{\frac{\lambda_n^2 - \bar{\beta}_m}{\bar{D}_m}} \tag{15}$$

Note that in the problem considered here, the reaction consumes the drug, and therefore, $\bar{\beta}_m$ is always positive. In contrast, the reaction coefficient in similar diffusion-reaction heat transfer problems may be either positive or negative, depending on whether the reaction is endothermic or exothermic [9]. The implications of a positive value of $\bar{\beta}_m$ on imaginary eigenvalues in this problem are considered later in Section 4.

Now, the boundary and interface conditions given by Eqs. (8)-(11) are used to determine the unknown coefficients $A_{m,n}$ and $B_{m,n}$, as well as the eigenvalues λ_n. By substituting Eq. (13) in Eqs. (8)-(11), one may obtain

$$A_{1,n} = 0 \tag{16}$$

$$\omega_{M,n}[-A_{M,n}\sin\omega_{M,n} + B_{M,n}\cos\omega_{M,n}] = (1 - Sh)[A_{M,n}\cos\omega_{M,n} + B_{M,n}\sin\omega_{M,n}] \tag{17}$$

$$A_{m+1,n}\cos(\omega_{m+1,n}\gamma_m) + B_{m+1,n}\sin(\omega_{m+1,n}\gamma_m) = \sigma_m[A_{m,n}\cos(\omega_{m,n}\gamma_m) + B_{m,n}\sin(\omega_{m,n}\gamma_m)] \quad m = 1, 2 \ldots M - 1 \tag{18}$$

$$\begin{aligned}
\bar{D}_m[&-A_{m,n}\cos(\omega_{m,n}\gamma_m) - B_{m,n}\sin(\omega_{m,n}\gamma_m) + \omega_{m,n}\gamma_m[-A_{m,n}\sin(\omega_{m,n}\gamma_m) + B_{m,n}\cos(\omega_{m,n}\gamma_m)]] \\
&= \bar{D}_{m+1}[-A_{m+1,n}\cos(\omega_{m+1,n}\gamma_m) - B_{m+1,n}\sin(\omega_{m+1,n}\gamma_m) + \omega_{m+1,n}\gamma_m[-A_{m+1,n}\sin(\omega_{m+1,n}\gamma_m) + B_{m+1,n}\cos(\omega_{m+1,n}\gamma_m)]] \\
&m = 1, 2 \ldots M - 1
\end{aligned} \tag{19}$$

Eqs. (16)-(19) constitute $2M$ equations in $2M$ unknown variables $A_{m,n}$ and $B_{m,n}$ ($m = 1,2..M$). Since these equations are homogeneous, one must require the determinant of this set of equations to be zero in order to ensure a non-trivial solution. It also follows that one of the equations becomes redundant. The requirement of zero determinant results in the eigenequation needed to determine the eigenvalues λ_n. A formal derivation of the eigenequation, and coefficients $A_{m,n}$ and $B_{m,n}$ is presented in Appendix A, which shows that the eigenequation for the general M-layer problem is given by:

$$\begin{aligned}
&\frac{\bar{D}_M\sigma_{M-1}q_{M-1,n}(\gamma_{M-1})[\omega_{M,n}\cot(\omega_{M,n}\gamma_{M-1})\gamma_{M-1} - 1] - \bar{D}_{M-1}\dot{q}_{M-1,n}(\gamma_{M-1})\gamma_{M-1}}{\bar{D}_M\sigma_{M-1}q_{M-1,n}(\gamma_{M-1})[\omega_{M,n}\gamma_{M-1} + \cot(\omega_{M,n}\gamma_{M-1})] + \bar{D}_{M-1}\dot{q}_{M-1,n}(\gamma_{M-1})\cot(\omega_{M,n}\gamma_{M-1})\gamma_{M-1}} \\
&\quad + \frac{1 - \omega_{M,n}\cot(\omega_{M,n}) - Sh}{\cot(\omega_{M,n}) + \omega_{M,n} - Sh \cdot \cot(\omega_{M,n})} = 0
\end{aligned} \tag{20}$$

where $q_{m,n}(\xi)$ is given in Appendix A. and over-dot denotes the derivative with respect to ξm.

Once the eigenvalues and coefficients are determined, the initial condition given by Eq. (12) may be written as

$$\theta_{m,in}(\xi) = \sum_{n=1}^{\infty} g_n \left[A_{m,n} \frac{\cos(\omega_{m,n}\xi)}{\xi} + B_{m,n} \frac{\sin(\omega_{m,n}\xi)}{\xi} \right] \tag{21}$$

The coefficients g_n may be determined by using the principle of quasi-orthogonality of multi-layer eigenvalues. Specifically, for each layer m, Eq. (21) is multiplied by $\xi^2[A_{m,n'} \frac{\cos(\omega_{m,n'}\xi)}{\xi} + B_{m,n'} \frac{\sin(\omega_{m,n'}\xi)}{\xi}]$, followed by integration within the layer. The resulting equations are added, leading to the following expression for g_n

$$g_n = \frac{1}{N_n} \sum_{m=1}^{M} \int_{\gamma_{m-1}}^{\gamma_m} \xi^2 \theta_{m,in}(\xi) \left[A_{m,n} \frac{\cos(\omega_{m,n}\xi)}{\xi} + B_{m,n} \frac{\sin(\omega_{m,n}\xi)}{\xi} \right] d\xi \tag{22}$$

where the norm N_n is given by

$$N_n = \sum_{m=1}^{M} \int_{\gamma_{m-1}}^{\gamma_m} [A_{m,n}\cos(\omega_{m,n}\xi) + B_{m,n}\sin(\omega_{m,n}\xi)]^2 d\xi \tag{23}$$

Note that in many practical cases, the drug is loaded uniformly only in the core, i.e., $\theta_{m,in} = 1$ for $m = 1$, $\theta_{m,in} = 0$ for $m = 2,3,M$. This leads to significant simplification in Eq. (22).

2.4. Drug delivery performance parameters

A key parameter of interest is the cumulative fraction of drug released as a function of time. This may be obtained by integrating the concentration flux at the outer surface over time, and normalizing with respect to the initial drug loaded in the capsule. In non-dimensional form, this quantity is given by

$$\overline{\psi}(\tau) = \frac{\int_0^{\tau} \left(\frac{\partial\theta_M}{\partial\xi} \right)_{\xi=1} d\tau}{\sum_{m=1}^{M} \int_{\gamma_{m-1}}^{\gamma_m} \xi^2 \theta_{m,in}(\xi) d\xi} \tag{24}$$

Note that $\bar{\psi}(\tau)$ is expected to increase with time and saturate asymptotically at large time. In the absence of reaction $(\bar{\beta}_m = 0)$, $\bar{\psi}(\tau) \to 1$ at large time, i.e., all drug eventually diffuses out of the multilayer sphere. However, for $\bar{\beta}_m > 0$, $\bar{\psi}(\tau)$ is expected to saturate at a value lower than 1 as some of the drug is absorbed due to reaction and can never be released. Further, note that in principle, complete release is achieved only at infinite time. Therefore, it is helpful to define a release time as the time by which the drug delivered, $\bar{\psi}(\tau)$, is a fraction close to 1, say 0.95.

Another parameter of interest, particularly due to the presence of drug absorption within each layer, is the total mass of drug absorbed due to reaction within each layer. This can be expressed as a fraction of the initial drug loading as follows

$$\bar{\chi}_m(\tau) = \frac{\int_0^\tau \int_{\gamma_{m-1}}^{\gamma_m} \xi^2 \bar{\beta}_m \theta_m(\xi, t) d\xi d\tau}{\sum\limits_{m=1}^{M} \int_{\gamma_{m-1}}^{\gamma_m} \xi^2 \theta_{m,in}(\xi) d\xi} \tag{25}$$

Finally, the mass of drug remaining in each layer at any time can be expressed as a fraction of the initial drug loading as follows:

$$\bar{\rho}_m(\tau) = \frac{\int_{\gamma_{m-1}}^{\gamma_m} \xi^2 \theta_m(\xi, \tau) d\xi}{\sum\limits_{m=1}^{M} \int_{\gamma_{m-1}}^{\gamma_m} \xi^2 \theta_{m,in}(\xi) d\xi} \tag{26}$$

The quantities $\bar{\psi}(\tau)$, $\bar{\chi}_m(\tau)$ and $\bar{\rho}_m(\tau)$ can be shown to be related to each other as follows: One may multiply the governing equation for each layer (Eq. (7)) by ξ^2, integrate within each layer, and add all the resulting equations. Further, integration over time followed by some simplification may be shown to result in

$$\bar{\psi}(\tau) + \sum_{m=1}^{M} \bar{\chi}_m(\tau) + \sum_{m=1}^{M} \bar{\rho}_m(\tau) = 1 \tag{27}$$

which may be interpreted as a statement of overall mass balance in the system.

2.5. Modeling of a thin coating on the outer surface

Finally, a resistance-based technique for modeling the impact of a thin coating on the outer surface of the sphere is described. A thin coating is often provided for chemical stability and to control the drug release characteristics [4,5]. When the coating is relatively thin, it may not be practical to treat it as a separate layer in the multi-layer problem. Instead, one may add the mass transfer resistance offered by the thin coating to the convective resistance on the outer surface, in order to model the impact of the thin coating on the diffusion-reaction problem. Assuming that the thickness and diffusion coefficient of the thin coating are l and D_c, respectively, one may write the following modified boundary condition on the outer surface instead of Eq. (3)

$$-D_M \left(\frac{\partial c_M}{\partial r} \right)_{r=R_M} = \frac{(c_M)_{r=R_M}}{\frac{1}{h} + \frac{l}{D_c}} \tag{28}$$

which, in non-dimensional form may be written as

$$-\left(\frac{\partial \theta_M}{\partial \xi} \right)_{\xi=1} = Sh^*(\theta_M)_{\xi=1} \tag{29}$$

where, Sh^* is the modified Sherwood number, given by $\frac{1}{Sh*} = \frac{1}{Sh} + \frac{l}{R_M} \frac{D_M}{D_c}$. Therefore, the analysis presented so far remains valid for modeling the thin coating once Sh is replaced by Sh^*.

This treatment shows that accounting for the impact of the thin coating results in a reduction of the effective value of the Sherwood number at the outer surface. This effect is negligible if the non-dimensional parameter $\bar{g} = \frac{l}{R_M} \frac{D_M}{D_c} \ll \frac{1}{Sh}$, i.e., when the conduction resistance of the coating is much smaller than the convective resistance at the boundary. This could happen when $l \ll R_M$, i.e., a very thin coating, and/or $D_c \gg D_M$, i.e., a highly diffusive coating. On the other hand, when the coating is very thick, and/or poorly diffusive, one must explicitly account for the transient concentration distribution within the coating by considering it as one of the layers in the multilayer problem. Generally, the coating is quite thin, but of relatively low diffusivity. Therefore, whether the condition above is satisfied or not depends on the specific values of parameters in the problem.

The special case of a two-layer core-shell geometry is discussed next.

3. Special case – two-layer core-shell capsule

The commonly occurring case of a two-layer core-shell spherical capsule, in which the drug is initially loaded uniformly in the core is considered here. Previous works have presented analysis of this problem by considering only diffusion [22]. Here, the effect of reaction within the core and shell is also included. While the results for this case may be obtained by simply setting $M = 2$ in the previous section, it may be helpful to write these expressions explicitly, since the two-layer core-shell configuration occurs commonly. In this case, denoting the shell and core by 1 and 2, respectively, the governing equations for concentration distributions are given by Eq. (7) with $m = 1, 2$. Similarly, the boundary and interface conditions are given by equations (8), Eq. (9) with $M = 2$, and Eqs. (10) and (11) with $m = 1$. The initial condition for the problem is given by Eq. (12) with $m = 1, 2$.

With some mathematical simplification, it can be shown that a solution for the two-layer problem is given as follows:

$$\theta_1(\xi, \tau) = \sum_{n=1}^{\infty} g_n \frac{\sin(\omega_{1,n}\xi)}{\xi} \exp\left(-\lambda_n^2 \tau\right) \tag{30}$$

$$\theta_2(\xi, \tau) = \sum_{n=1}^{\infty} g_n s_n \left[p_n \frac{\cos(\omega_{2,n}\xi)}{\xi} + \frac{\sin(\omega_{2,n}\xi)}{\xi} \right] \exp\left(-\lambda_n^2 \tau\right) \tag{31}$$

where

$$p_n = \frac{-(1 - Sh)\sin(\omega_{2,n}) + \omega_{2,n}\cos(\omega_{2,n})}{(1 - Sh)\cos(\omega_{2,n}) + \omega_{2,n}\sin(\omega_{2,n})} \tag{32}$$

$$s_n = \frac{\sigma_1 \sin(\omega_{1,n}\gamma_1)}{p_n \cos(\omega_{2,n}\gamma_1) + \sin(\omega_{2,n}\gamma_1)} \tag{33}$$

and the eigenequation is given by

$$\bar{D}_1 \left[-\frac{1}{\gamma_1} + \omega_{1,n}\cot(\omega_{1,n}\gamma_1) \right] = \sigma_1 \left[-\frac{1}{\gamma_1} + \frac{\omega_{2,n}(-p_n + \cot(\omega_{2,n}\gamma_1))}{1 + p_n \cot(\omega_{2,n}\gamma_1)} \right] \tag{34}$$

Finally, the coefficients g_n are obtained from

$$g_n = \frac{\int_0^{\gamma_1} \xi \theta_{1,in}(\xi)\sin(\omega_{1,n}\xi)d\xi + \int_{\gamma_1}^1 \xi \theta_{2,in}(\xi)s_n(p_n \cos(\omega_{2,n}\xi) + \sin(\omega_{2,n}\xi))d\xi}{\int_0^{\gamma_1} \sin^2(\omega_{1,n}\xi)d\xi + \int_{\gamma_1}^1 [s_n(p_n \cos(\omega_{2,n}\xi) + \sin(\omega_{2,n}\xi))]^2 d\xi} \tag{35}$$

A few special cases of the two-layer problem are of interest. Firstly, in many cases, the drug is initially loaded uniformly only in the core. In such a case, $\theta_{2,in} = 0$, and therefore, the second term in the numerator in Eq. (35) can be removed. Another special case of interest is that of a zero concentration boundary at the outer surface ($Sh \to \infty$), for which, one may obtain

$$p_n = -\tan(\omega_{2,n}) \tag{36}$$

$$s_n = \frac{-\sigma_1 \sin(\omega_{1,n}\gamma_1)\cos(\omega_{2,n})}{\sin(\omega_{2,n}(1 - \gamma_1))} \tag{37}$$

It is of interest to write explicit expressions for the key parameters to characterize the nature of drug delivery from the two-layer core-shell capsule. For an initial uniform loading of c_{in} in the core, the cumulative drug released as a function of time is given by

$$\overline{\psi}(\tau) = \frac{3}{\gamma_1^3} \int_0^{\tau} -\left(\frac{\partial \theta_2}{\partial \xi}\right)_{\xi=1} d\tau = -\frac{3}{\gamma_1^3} \sum_{n=1}^{\infty} g_n s_n [(\omega_{2,n} - p_n)(\cos(\omega_{2,n}) - (1 + \omega_{2,n}p_n)\sin(\omega_{2,n}))] \frac{(1 - \exp(-\lambda_n^2 \tau))}{\lambda_n^2} \tag{38}$$

The mass of drug absorbed in the core and shell due to reaction is given by

$$\bar{\chi}_1(\tau) = \frac{3}{\gamma_1^3} \int_0^{\tau} \int_0^{\gamma_1} \xi^2 \bar{\beta}_1 \theta_1(\xi, \tau) d\xi d\tau = \frac{3\bar{\beta}_1}{\gamma_1^3} \sum_{n=1}^{\infty} g_n \left[\frac{\sin(\omega_{1,n}\gamma_1) - \omega_{1,n}\gamma_1 \cos(\omega_{1,n}\gamma_1)}{\omega_{1,n}^2} \right] \frac{(1 - \exp(-\lambda_n^2 \tau))}{\lambda_n^2} \tag{39}$$

$$\bar{\chi}_2(\tau) = \frac{3\bar{\beta}_2}{\gamma_1^3} \int_0^{\tau} \int_{\gamma_1}^1 \xi^2 \bar{\beta}_2 \theta_2(\xi, \tau) d\xi d\tau = \frac{3}{\gamma_1^3} \sum_{n=1}^{\infty} \frac{g_n s_n}{\omega_{2,n}^2} [(p_n \omega_{2,n} + 1)\sin(\omega_{2,n})$$
$$+ (p_n - \omega_{2,n})\cos(\omega_{2,n}) - (p_n \omega_{2,n}\gamma_1 + 1)\sin(\omega_{2,n}\gamma_1) + (\omega_{2,n}\gamma_1 - p_n)\cos(\omega_{2,n}\gamma_1)] \frac{(1 - exp(-\lambda_n^2 \tau))}{\lambda_n^2} \tag{40}$$

Finally, the fraction of drug remaining in the core and shell at any time, relative to the original drug loading is given by

$$\bar{\rho}_1(\tau) = \frac{3}{\gamma_1^3} \int_0^{\gamma_1} \xi^2 \theta_1(\xi, \tau) d\xi = \frac{3}{\gamma_1^3} \sum_{n=1}^{\infty} g_n \left[\frac{\sin(\omega_{1,n}\gamma_1) - \omega_{1,n}\gamma_1 \cos(\omega_{1,n}\gamma_1)}{\omega_{1,n}^2} \right] \exp(-\lambda_n^2 \tau) \tag{41}$$

$$\overline{\rho}_2(\tau) = \frac{3}{\gamma_1^3} \int_{\gamma_1}^1 \xi^2 \theta_2(\xi, \tau) d\xi = \frac{3}{\gamma_1^3} \sum_{n=1}^{\infty} \frac{g_n s_n}{\omega_{2,n}^2} [(p_n \omega_{2,n} + 1)\sin(\omega_{2,n}) + (p_n - \omega_{2,n})\cos(\omega_{2,n})$$
$$- (p_n \omega_{2,n}\gamma_1 + 1)\sin(\omega_{2,n}\gamma_1) + (\omega_{2,n}\gamma_1 - p_n)\cos(\omega_{2,n}\gamma_1)] \exp\left(-\lambda_n^2 \tau\right) \tag{42}$$

The overall mass balance for the two-layer problem requires that at any time

$$\bar{\psi}(\tau) + \bar{\chi}_1(\tau) + \bar{\chi}_2(\tau) + \bar{\rho}_1(\tau) + \bar{\rho}_2(\tau) = 1 \tag{43}$$

4. Imaginary eigenvalue analysis

Previous work has shown that multilayer diffusion-reaction problems may admit imaginary eigenvalues, even if the problem is one-dimensional [9, 20]. Therefore, it is important to analyze and understand if imaginary eigenvalues may arise in the present problem. In addition to theoretical interest in imaginary eigenvalues, such an analysis is also practically important, because imaginary eigenvalues may be associated with divergence of the series solution at large time, and standard eigenvalue computation algorithms may not find an imaginary eigenvalue. While the analysis below is presented for a two-layer problem for simplicity, similar results apply for the general M-layer case.

For the infinite sink boundary condition, $Sh \rightarrow \infty$, the following analysis proves that when the Damköhler numbers $\bar{\beta}_1$ and $\bar{\beta}_2$ are both positive, as is the case in the present problem, the eigenvalues λ_n must all be real.

Consider the eigenequation for $Sh \rightarrow \infty$

$$f(\lambda^2) = \bar{D}_1 \left[-\frac{1}{\gamma_1} + \omega_1 \cot(\omega_1 \gamma_1) \right] + \sigma_1 \left[\frac{1}{\gamma_1} + \omega_2 \cot(\omega_2(1-\gamma_1)) \right] = 0 \tag{44}$$

where ω_1 and ω_2 are given by Eq. (15).

In order to prove that Eq. (44) does not admit an imaginary root, it is sufficient to prove that

(a) $f(0) > 0$, and
(b) $f(\lambda^2)$ increases monotonically as λ^2 decreases.

(a) and (b) together ensure that $f(\lambda^2)$ never crosses the x-axis for $\lambda^2 < 0$, and therefore, does not have an imaginary root. In order to prove (a), one may set $\lambda^2 = 0$ in Eq. (44), which results in

$$f(0) = \bar{D}_1 \left[-\frac{1}{\gamma_1} + \sqrt{\frac{\bar{\beta}_1}{\bar{D}_1}} \coth\left(\sqrt{\frac{\bar{\beta}_1}{\bar{D}_1}} \gamma_1\right) \right] + \sigma_1 \left[\frac{1}{\gamma_1} + \sqrt{\bar{\beta}_2} \coth\left(\sqrt{\bar{\beta}_2}(1-\gamma_1)\right) \right] \tag{45}$$

Now, the second term on the right hand side of Eq. (45) is always positive, since $\bar{\beta}_2 > 0$ and $(1-\gamma_1) > 0$ in the present problem, and $\coth(x) > 0$ for real, positive x. Further, the first term on the right hand side in Eq. (45) may be written as $\frac{\bar{D}_1}{\gamma_1}[-1 + x \coth(x)]$, where $x = \sqrt{\frac{\bar{\beta}_1}{\bar{D}_1}}\gamma_1$. Now, since $\bar{\beta}_1 > 0$ in the present problem, and $x \coth(x) > 1$ for real, positive x, therefore, the first term on the right hand side in Eq. (45) is also positive. This proves that $f(0) > 0$ when $\bar{\beta}_1 > 0$ and $\bar{\beta}_2 > 0$.

In order to prove (b), Eq. (44) is re-written in terms of the imaginary complement, $\hat{\lambda} = i\lambda$, where $i = \sqrt{-1}$ is the unit imaginary number. This results in

$$f(\hat{\lambda}^2) = \bar{D}_1 \left[-\frac{1}{\gamma_1} + \hat{\omega}_1 \coth(\hat{\omega}_1 \gamma_1) \right] + \sigma_1 \left[\frac{1}{\gamma_1} + \hat{\omega}_2 \coth(\hat{\omega}_2(1-\gamma_1)) \right] \tag{46}$$

where

$$\hat{\omega}_1 = \sqrt{\frac{\hat{\lambda}^2 + \bar{\beta}_1}{\bar{D}_1}}; \quad \hat{\omega}_2 = \sqrt{\hat{\lambda}^2 + \bar{\beta}_2} \tag{47}$$

In order to prove (b), it is sufficient to prove that $\frac{df}{d\hat{\lambda}} > 0$ for $\hat{\lambda} > 0$. Eq. (46) is differentiated to result in
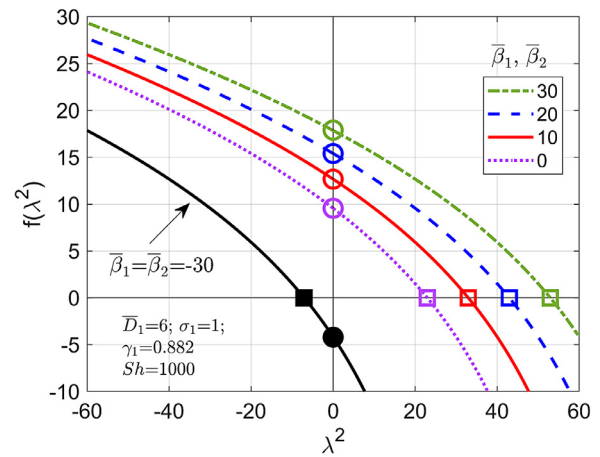

Fig. 2. Eigenfunction plot in both real and imaginary spaces to illustrate the impact of Damköhler numbers on the nature of eigenvalues. Plot parameters are $\bar{D}_1 = 6$; $\sigma_1 = 1$; $\gamma_1 = 0.882$; $Sh = 1000$. Square markers indicate the first eigenvalue. Circular markers indicate the value of the eigenfunction at the transition between real and imaginary eigenvalues, $\lambda^2 = 0$. A case of negative Damköhler number is also shown for illustration of a case of imaginary eigenvalues.

$$\frac{df}{d\hat{\lambda}} = \sqrt{\frac{\bar{D}_1}{\hat{\lambda}^2 + \bar{\beta}_1}} \hat{\lambda} \frac{\partial}{\partial \hat{\omega}_1} \left(\hat{\omega}_1 \coth(\hat{\omega}_1 \gamma_1)\right)$$
$$+ \sigma_1 \sqrt{\frac{1}{\hat{\lambda}^2 + \bar{\beta}_1}} \hat{\lambda} \frac{\partial}{\partial \hat{\omega}_2} \left(\hat{\omega}_2 \coth(\hat{\omega}_2(1-\gamma_1))\right) \tag{48}$$

Now,

$$\frac{\partial}{\partial \hat{\omega}_1} \left(\hat{\omega}_1 \coth(\hat{\omega}_1 \gamma_1)\right) = \frac{1}{2} \text{csch}^2(\hat{\omega}_1 \gamma_1) \left(\sinh(2\hat{\omega}_1 \gamma_1) - 2\hat{\omega}_1 \gamma_1\right)$$
$$= \frac{1}{2} \text{csch}^2(\hat{\omega}_1 \gamma_1) \left(\frac{(2\hat{\omega}_1 \gamma_1)^3}{3!} + \frac{(2\hat{\omega}_1 \gamma_1)^5}{5!} + ..\right) > 0 \tag{49}$$

This proves that $\frac{df}{d\hat{\lambda}} > 0$ for $\hat{\lambda} > 0$, and therefore statement (b) is true. Therefore, the present problem, with $\bar{\beta}_1 > 0$ and $\bar{\beta}_2 > 0$ admits only real eigenvalues.

In order to illustrate the mathematical proof presented above, Fig. 2 presents plots of the eigenfunction close to $\lambda^2 = 0$. The plot is presented in both real ($\lambda^2 > 0$) and imaginary ($\lambda^2 < 0$) regions for several positive values of $\bar{\beta}_1$ and $\bar{\beta}_2$. The value of the eigenfunction at $\lambda^2 = 0$ and the first eigenvalue for each case are indicated by circular and square symbols, respectively. The plot clearly shows, as predicted by the proof presented above, that $f(\lambda^2 = 0) > 0$ in each case, including the limiting case of $\bar{\beta}_1 = \bar{\beta}_2 = 0$, as shown by circular symbols, and that $f(\lambda^2)$ is a monotonically increasing function as the magnitude of λ^2 increases in the imaginary region ($\lambda^2 < 0$). As a result, the eigenfunction curve never crosses the x axis in the imaginary region, and therefore, there is no possibility of an imaginary eigenvalue. In contrast, a case of negative $\bar{\beta}_1$ and $\bar{\beta}_2$ corresponding to a species-generating reaction term is also plotted in Fig. 2 for illustration. In this case, while $f(\lambda^2)$ is still a monotonically increasing function as the magnitude of λ^2 increases in the imaginary region, however, $f(\lambda^2 = 0) < 0$, and therefore, the eigenfunction must cross the negative x-axis, resulting in the existence of an imaginary eigenvalue.

The physical interpretation of this result is related to the absorptive nature of the reaction term when $\bar{\beta}_1 > 0$ and $\bar{\beta}_2 > 0$. In such a case, the drug is absorbed by reaction throughout the domain, and there is no likelihood of a reaction-driven build-up of drug that may lead to divergence of the drug concentration distribution. In contrast, in a thermal diffusion-reaction problem involving an exothermic reaction (i.e. $\bar{\beta}_1$ and $\bar{\beta}_2$ may be negative), imaginary eigenvalues have been shown to exist [9]. This is because in

Table 1
Reference parameter values for diffusivities, radii and drug partition coefficient.

Parameter	Value	Reference
D_1	30×10^{-11} m^{2}s^{-1}	[30]
D_2	5×10^{-11} m^{2}s^{-1}	[30]
R_1	1.5×10^{-3} m	[22]
R_2	1.7×10^{-3} m	[22]
σ_1	1	[22]

such a case, heat is generated proportional to the local temperature, leading to temperature rise, which may further increase the heat generated, eventually leading to thermal runaway. In contrast, this is not a concern in the present problem where the reaction term results in absorption, not generation of the drug.

Note that according to Eq. (15), $\omega_{1,n}$ and/or $\omega_{2,n}$ may become imaginary even if λ_n is real, for example, when $\bar{\beta}_1$ and/or $\bar{\beta}_2$ is large and positive. However, this does not present a problem. For example, if $\omega_{1,n}$ is real and $\omega_{2,n}$ is imaginary, then, p_n is imaginary, s_n is imaginary and hence g_n remains real, according to Eqs. (32), (33) and (35), respectively. Therefore, from Eqs. (30) and (31), the concentration distributions θ_1 and θ_2 remain real. Similarly, for each of the other three cases, it can be shown that the concentration distributions θ_1 and θ_2 remain real regardless of the nature of $\omega_{1,n}$ and $\omega_{2,n}$.

5. Results and discussion

This section discusses a number of results based on the analytical model presented in Sections 2 and 3. The values of various parameters in the problem are taken from the literature, and are summarized in Table 1. Specifically, diffusion coefficients in the core and shell are taken from past measurements [30]. A representative geometry of the core-shell structure and value of the drug partition coefficient is also assumed, based on previous work [22]. There is a relative lack of literature to estimate the values of $\bar{\beta}_1$ and $\bar{\beta}_2$. Based on parameter estimation using experimental data and a numerical simulation model, Pontrelli, et al. have reported Damköhler numbers for the chemotherapeutic agent daunorubicin and [Cu(TPMA) (Phenantroline)] (ClO4)$_2$, a common metallodrug [8]. Their data suggests strong pH dependence of $\bar{\beta}_1$ and $\bar{\beta}_2$, with values ranging from 0.1 to 10.9. Given the strong pH dependence, representative values within this range are chosen for the present analysis. Further, *Sh* can, in general, vary between zero (impenetrable boundary) to infinity (infinite sink). A number of different values of *Sh* are considered in the analysis presented here.

Prior to analysis of this problem, it is important to note that since the analytical solution derived here is in the form of an infinite series solution, it must, in practice, be truncated to a finite number of terms for computation. Therefore, the effect of number of terms on accuracy must be established. Fig. 3(a) plots concentration at two specific points in the core and shell as functions of time for 1, 3, 10 and 100 terms in Eqs. (30) and (31). These plots show good convergence with ten terms. Curves corresponding to ten terms are nearly coincident with those corresponding to hundred terms. Numerical data for concentration at two locations, and at four different times are listed for different number of eigenvalues (1, 3, 10 and 100) are summarized in Table 2. Computed data for 10 and 100 terms are identical up to 16 decimals.

For the same problem, Fig. 3(b) plots the mass of drug released as a function of time, as predicted by Eq. (38) with 1, 3, 10 and 100 terms. Similar to Fig. 3(a), these plots show good convergence of the series solution within ten terms. Numerical data for $\bar{\psi}(\tau)$ for different number of eigenvalues are presented in Table 3. These

data supplement Figs. 3(a) and 3(b) in establishing convergence with ten terms.

Note that the error incurred by the use of only one term is around 10.7% at $\tau = 0.3$, which may be acceptable for some engineering applications. Since the computational time involved in the series terms is negligible, all plots presented in this work are computed with ten terms to ensure good accuracy. Note that eigenvalues are computed using an algorithm that discretizes and carries out a root search based on Newton-Raphson method in regions where the eigenequation curve crosses the *x*-axis. The first ten eigenvalues determined for this problem are listed in Table 4.

Comparison of the theoretical model presented here with past work based on numerical simulations [22] is carried out next. In this past work, diffusion in a two-layer spherical structure with the environment around the sphere considered as a third layer was numerically computed. No reaction was modeled and the initial drug concentration was assumed to exist only in the inner-most layer. Using the parameters presented in this paper, concentration distributions at different times and amount of drug remaining as function of time are computed and compared with numerical calculations presented in the past work, as shown in Figs. 4(a) and 4(b), respectively. In both cases, there is very good agreement between the present theoretical work and the past numerical study. Note that the present work is a significant generalization of the three-layer geometry considered in the past work. In addition to generalizing to an arbitrary number of layers, the present work also accounts for a reaction term in each layer. Moreover, closed-form analytical solutions presented in this work are preferable over numerical solutions both for theoretical elegance, as well as for practical ease of implementation.

The first ten eigenvalues determined for this problem are listed in Table 4.

Fig. 5 presents a plot of the various performance parameters of interest for a representative problem. For the parameter values listed in Table 1, and with *Sh* = 10, Fig. 5 plots the cumulative mass of drug released, $\bar{\psi}(\tau)$, cumulative mass of drug absorbed in core and shell, $\bar{\chi}_1(\tau)$ and $\bar{\chi}_2(\tau)$, respectively, and the mass of drug remaining in core and shell, $\bar{\rho}_1(\tau)$ and $\bar{\rho}_2(\tau)$, respectively. Plots are presented for cases with reaction ($\bar{\beta}_1 = \bar{\beta}_2 = 4$) and without reaction ($\bar{\beta}_1 = \bar{\beta}_2 = 0$) in Figs. 5(a) and 5(b), respectively. $\bar{\beta}_1$ and $\bar{\beta}_2$ are assumed to be equal to each other for simplicity, although the model is capable of considering different values for the two. There is a very short initial period, not clearly visible in Fig. 5, where $\bar{\psi}(\tau)$ does not rise appreciably. This corresponds to the period during which the drug is still diffusing through the core/shell. Beyond this short period, both Figures show a gradual increase in the cumulative amount of drug released, followed by plateauing out at large time. The mass of drug remaining in the core, $\bar{\rho}_1(\tau)$ starts at a value of 1 at $t = 0$, representing all of the drug being present in the core at $t = 0$. As time passes, $\bar{\rho}_1(\tau)$ decreases towards 0 at large time, which is because of drug diffusion from the core into the shell. On the other hand, the mass of drug remaining in the shell, $\bar{\rho}_2(\tau)$ starts at zero, rises rapidly at first, due to diffusion from the core, and then gradually decays away, as drug released from the outer surface of the shell outweighs drug diffusing into the shell from the core. The cumulative mass of drug absorbed in the core and shell – $\bar{\chi}_1(\tau)$ and $\bar{\chi}_2(\tau)$, respectively – rises with time, but as the drug concentration in the core and shell itself reduces, $\bar{\chi}_1(\tau)$ and $\bar{\chi}_2(\tau)$ also reach a terminal value. At large times, all of the initial drug has been either released into the outside or absorbed in reactions in the core and shell. As expected, and as shown in Fig. 5(b), when $\bar{\beta}_1 = \bar{\beta}_2 = 0$, corresponding to no reaction, $\bar{\chi}_1(\tau)$ and $\bar{\chi}_2(\tau)$ are both zero throughout, and all of the initial drug loading is released into the release medium. In contrast, a non-zero value of $\bar{\beta}_1$ and $\bar{\beta}_2$ results in a reduced mass of total drug released. For both cases, however, as expected, the sum of
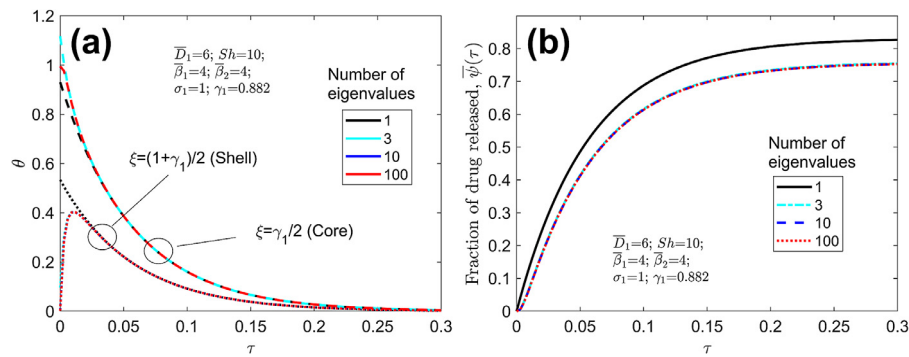
Fig. 3. Effect of number of eigenvalues on (a) Concentration distributions at $\xi = \gamma_1/2$ (core) and $\xi = (1 + \gamma_1)/2$ (shell) as functions of τ; (b) fraction of drug released, $\bar{\psi}(\tau)$ as a function of τ. Other problem parameters are $\bar{D}_1 = 6$; $Sh = 10$; $\bar{\beta}_1 = \bar{\beta}_2 = 4$; $\sigma_1 = 1$; $\gamma_1 = 0.882$.

Table 2
Computed values of concentrations at $\xi = \gamma_1/2$ (core) and $\xi = (1 + \gamma_1)/2$ (shell) at four different times for 1, 3, 10 and 100 eigenvalues. Problem parameters correspond to Fig. 3.

	Number of eigenvalues				% difference between results with 10 and 100 eigenvalues
τ	1	3	10	100	
0.05	0.386392505503835, 0.221663550290146	0.386560795345826, 0.221557273250833	0.386560795345171, 0.221557273250529	0.386560795345171, 0.221557273250529	0, 0
0.10	0.160465228465379, 0.092054819213884	0.160465379196044, 0.092054724085412	0.160465379196044, 0.092054724085412	0.160465379196044, 0.092054724085412	0, 0
0.20	0.027674859703704, 0.015876362942666	0.027674859703825, 0.015876362942589	0.027674859703825, 0.015876362942589	0.027674859703825, 0.015876362942589	0, 0
0.30	0.004772983324453, 0.002738139104935	0.004772983324453, 0.002738139104935	0.004772983324453, 0.002738139104935	0.004772983324453, 0.002738139104935	0, 0

Table 3
Computed values of $\bar{\psi}(\tau)$ at four different times for 1, 3, 10 and 100 eigenvalues. Problem parameters correspond to Fig. 3.

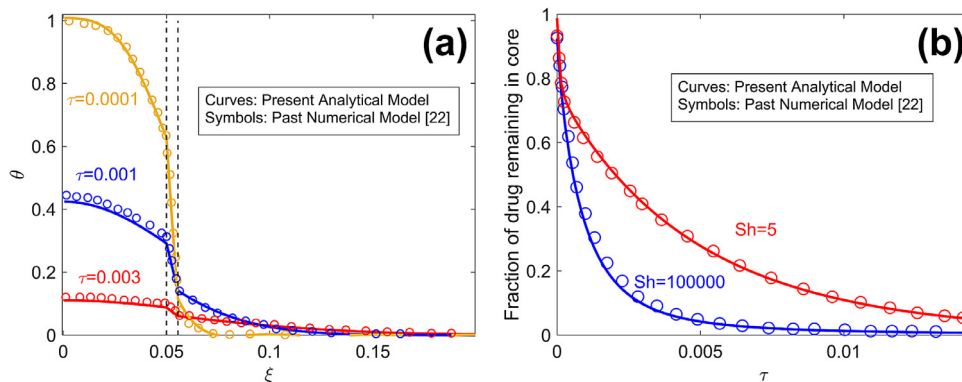|	Number of eigenvalues			
τ	1	3	10	100
0.05	0.485963075193943	0.414093980013804	0.412016046158976	0.411420906143879
0.10	0.687779038950933	0.615885310703228	0.613807376848360	0.613212236833263
0.20	0.806397811330161	0.734504061008142	0.732426127153275	0.731830987138177
0.30	0.826855563549852	0.754961813227815	0.752883879372948	0.752288739357850

Fig. 4. Comparison of the present theoretical model with past numerical model [22] for a three-layer problem: (a) concentration distribution at three different times with $Sh = 100,000$; (b) fraction of drug remaining in core as a function of time for two different values of Sh. Consistent with past work, the values of other parameters are $\bar{D}_1 = 1$; $\bar{D}_2 = 0.167$; $\sigma_1 = 1$; $\gamma_1 = 0.05$; $\gamma_2 = 0.056$.

$\bar{\psi}(\tau)$, $\bar{\chi}_1(\tau)$, $\bar{\chi}_2(\tau)$, $\bar{\rho}_1(\tau)$ and $\bar{\rho}_2(\tau)$ is one at all times, in keeping with conservation of mass as governed by Eq. (43).

Figs. 6(a) and 6(b) plot illustrative concentration distribution curves at multiple times in the core-shell composite with and without reaction, respectively. Starting at $t = 0$ with a uniform concentration of 1 and 0 in the core and shell, respectively, these plots show gradual decay of the concentration distribution in the core. On the other hand, concentration distribution in the shell in-

creases first, as the drug diffuses into the shell from the core, and then decreases once the drug begins to release into the outside medium. At large times, as expected, the drug concentration profiles in both core and shell decay to zero.

The Sherwood number, Sh, and Damköhler numbers, $\bar{\beta}_1$ and $\bar{\beta}_2$ play a key role in determining the nature of drug release in this problem. The impact of Sh on the drug release process is investigated in Fig. 7. The cumulative amount of drug released is plotted
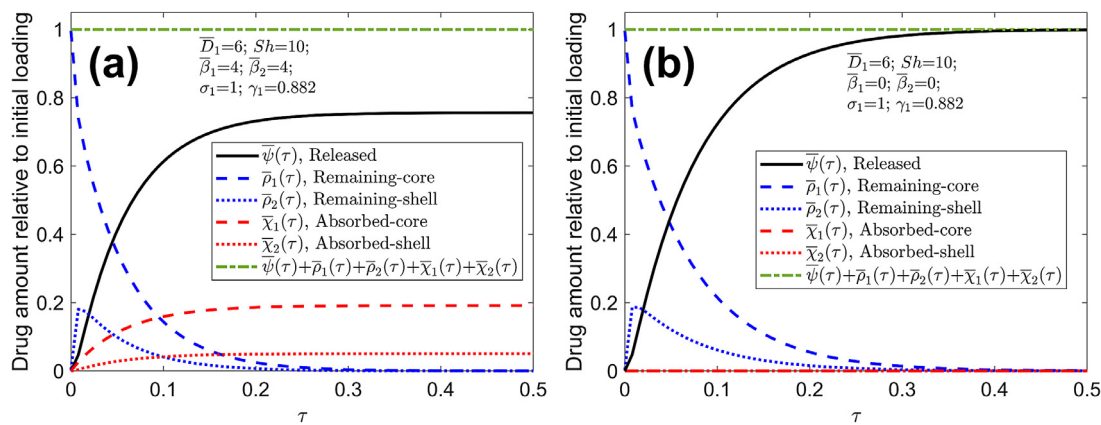
Fig. 5. Drug released, remaining and absorbed as functions of time for (a) $\bar{\beta}_1 = \bar{\beta}_2 = 4$; (b) $\bar{\beta}_1 = \bar{\beta}_2 = 0$ (no reaction) cases. Other problem parameters are $\bar{D}_1 = 6$; $Sh = 10$; $\sigma_1 = 1$; $\gamma_1 = 0.882$.
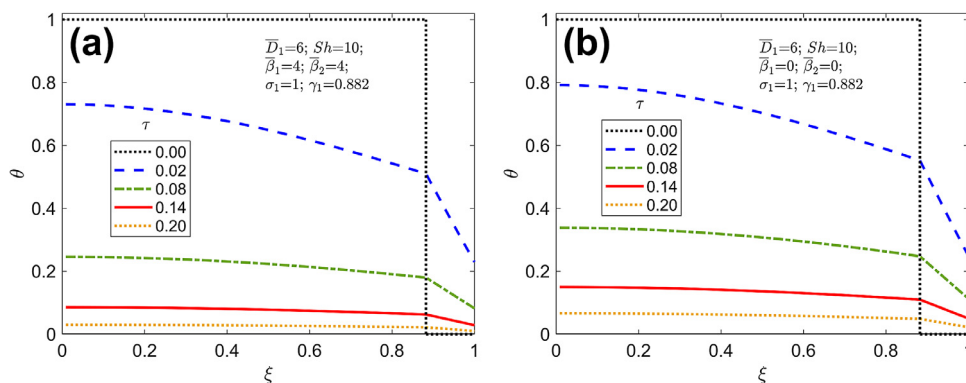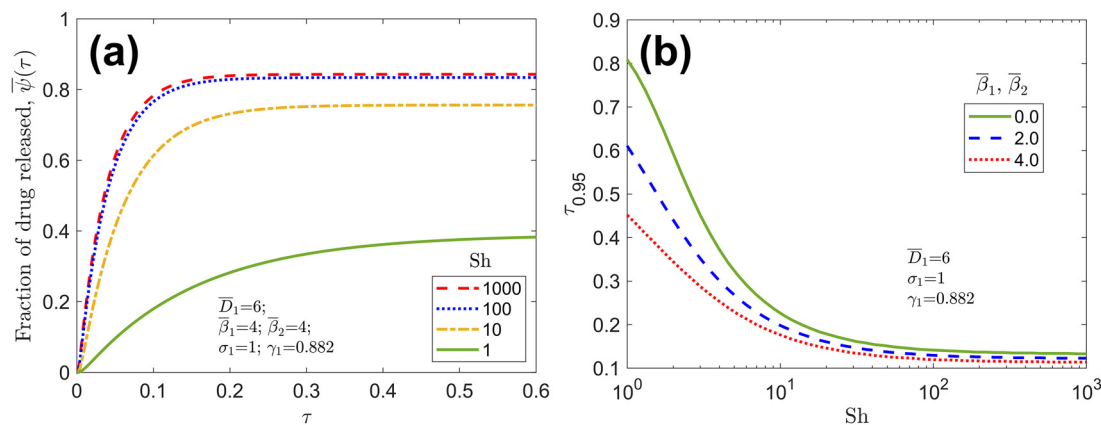

Fig. 6. Illustrative concentration distribution plots: θ_1 and θ_2 as functions of ξ at multiple times for (a) $\bar{\beta}_1 = \bar{\beta}_2 = 4$; (b) $\bar{\beta}_1 = \bar{\beta}_2 = 0$ (no reaction) cases. Other problem parameters are $\bar{D}_1 = 6$; $Sh = 10$; $\sigma_1 = 1$; $\gamma_1 = 0.882$.

Fig. 7. Effect of Sherwood number: (a) $\bar{\psi}(\tau)$ as a function of τ for multiple values of Sh; (b) time taken to deliver 95% of the eventual dose delivered as a function of Sh for three different values of $\bar{\beta}_1$ and $\bar{\beta}_2$. Other problem parameters are $\bar{D}_1 = 6$; $\sigma_1 = 1$; $\gamma_1 = 0.882$. In addition, for part (a), $\bar{\beta}_1 = \bar{\beta}_2 = 4$.

as a function of time for four different values of Sh in Fig. 7(a). The lowest value considered here, $Sh = 1$, represents a very slow rate of release, which may be relevant, for example, when drug transport/clearance within the release medium is slow. On the other hand, as Sh increases, Fig. 7(a) shows increasingly faster drug release. A sufficiently high Sh essentially achieves an infinite sink condition. Saturation sets in around $Sh = 100$, beyond which, there is little change in the drug release profile with further increasing Sh. Therefore, in this case, a value of $Sh = 100$ or greater represents a perfect sink condition. Note that even in this case, not all of the drug is released because of the absorption reactions occurring within the core and shell that may entrap some of the drug

before it can be released at the outer surface. A low value of Sh not only reduces the rate at which the drug is released into the ambient, but also the total mass of drug released. This is because a low value of Sh increases the residence time of the drug inside the sphere before release, increasing the mass of drug available for reaction and thereby reducing the total mass of releasable drug.

Fig. 7(b) plots the time taken to release 95% of the drug as a function of Sh, which is representative of the release time of the drug. This is an important parameter to quantify the nature of drug release since drug release occurs asymptotically. It is seen that as Sh increases, the time taken to release decreases, as expected. Further, Fig. 7(b) also shows some dependence on the Damköh-
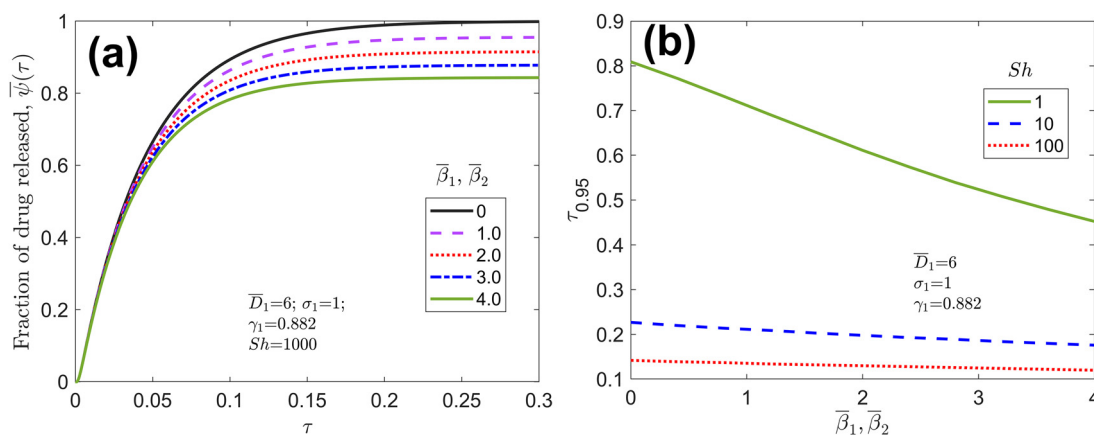
Fig. 8. Effect of Damköhler number: (a) $\bar{\psi}(\tau)$ as a function of τ for multiple values of $\bar{\beta}_1$ and $\bar{\beta}_2$; (b) time taken to deliver 95% of the eventual dose delivered as a function of $\bar{\beta}_1 = \bar{\beta}_2$ for three different values of Sh. Other problem parameters are $\bar{D}_1 = 6; \sigma_1 = 1; \gamma_1 = 0.882$. In addition, for part (a), $Sh = 1000$.

Table 4
Numerical values of first ten eigenvalues for the problems considered in Figs. 3 and 4.

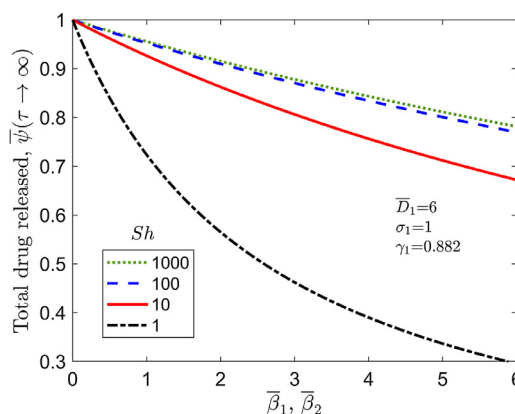|	λ_n	
n	Fig. 3	Fig. 4
1	4.192317813412143	3.141585288144737
2	11.847320121314180	6.282950128650931
3	17.539932046367877	9.422995368687273
4	22.838856910943637	12.558852940305355
5	30.244429357676854	15.684890369844636
6	37.524913153224276	18.791471185466413
7	42.860965183416816	21.863718979577946
8	48.850442642322449	24.882536952030190
9	56.394997248496004	27.835028641330229
10	63.632628469500020	30.739295191900858

Fig. 9. Effect of Damköhler number: Total drug released at large time as a function of $\bar{\beta}_1$ and $\bar{\beta}_2$ for four different values of Sh. Problem parameters are same as Fig. 8.

ler numbers, especially at low Sh. For the same Sherwood number, a high value of the Damköhler number results in more rapid completion of the release process. This is because a high value of Damköhler number contributes significantly towards entrapment of the available drug in the sphere. This effect is more prominent at small Sh, whereas at large Sh approaching constant concentration conditions on the outer surface, the time taken for release is not very sensitive to the Damköhler numbers.

Fig. 8 presents additional results to illustrate the impact of the Damköhler number on the drug release characteristics. Fig. 8(a) presents the cumulative fraction of drug released as a function of time for multiple values of the Damköhler number, assumed to be the same in both layers. The limiting case of $\bar{\beta}_1 = \bar{\beta}_2 = 0$ is also presented. Fig. 8(a) shows that as the Damköhler number increases, the mass of drug released steadily reduces. This is expected because an increased rate of reaction results in greater drug entrapment within the sphere. Fig. 8(a) is plotted for a very high value of Sh, for which, the total drug released decreases slightly with increasing Damköhler number.

Fig. 8(b) plots the time taken to release 95% of the drug as a function of Damköhler number, which is representative of the release time of the drug. It is seen that as the Damköhler number increases, the time taken to release decreases, as expected. The reduction is particularly steep at small values of Sh. When Sh is large, which may happen when the release medium around the capsule is very large, the release time is lower and relatively independent of the Damköhler number. This is primarily because of faster diffusion due to the infinite sink around the capsule at large Sh.

Further, Fig. 9 plots the total drug released from the sphere at large time as a function of the Damköhler number, for four dif-

ferent values of Sh, ranging from a low value, corresponding to very restrictive mass transfer at the boundary to a large value, corresponding to rapid mass transfer at the boundary. For large Sh, Fig. 9 shows small reduction in the drug released with increasing Damköhler number, consistent with Fig. 8(a). However, when Sh is relatively small, there is a rapid reduction in the drug released with increasing Damköhler number. This is because at small Sh, the drug residence time within the sphere is large, which results in greater absorption due to reaction, and, therefore, greater sensitivity of the total drug released to the reaction rate represented by the Damköhler number.

It is of interest to investigate the impact of the shell thickness on drug release characteristics. For this purpose, a drug-loaded core of fixed size of 1.5 mm radius is considered, and the drug release curve is computed using the theoretical model presented here for several different shell thicknesses, ranging from a very thin shell (5% of core radius) to a very thick shell (80% of core radius). All other parameters of the problem are held constant, including $h = 3.17 \times 10^{-5} \, ms^{-1}$ and $\bar{\beta}_1 = \bar{\beta}_2 = 8.06 \times 10^{-5} \, s^{-1}$ corresponding to $Sh = 1000$ and $\bar{\beta}_1 = \bar{\beta}_2 = 4.0$, respectively, for the smallest-sized sphere considered here. Other parameters are taken from Table 1. Fig. 10 shows that as the shell thickness increases, with core radius fixed, there is a gradual reduction both in the rate at which drug is released, as well as the total drug that is eventually released. This is because a thicker shell increases time for the drug to diffuse from the core to the outer surface. Additionally, this makes the drug available for absorption within the sphere for
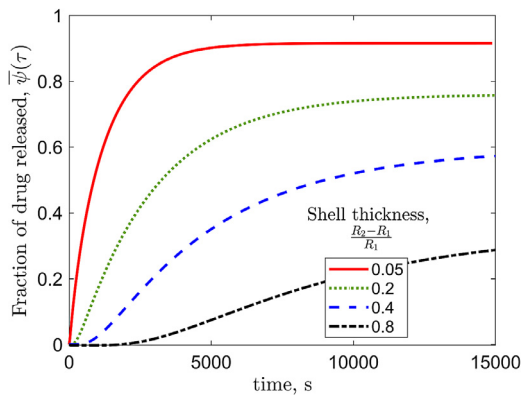
Fig. 10. Effect of shell thickness: $\bar{\psi}(\tau)$ as a function of dimensional time for multiple values of shell thickness $R_2 - R_1$ for a fixed core radius, $R_1 = 1.5$ mm. Other parameters are $D_1 = 30 \times 10^{-11}$ m^2s^{-1}; $D_2 = 5 \times 10^{-11}$ m^2s^{-1}; $h = 3.17 \times 10^{-5}$ ms^{-1}; $\sigma_1 = 1$; $\beta_1 = \beta_2 = 8.06 \times 10^{-5}$ s^{-1}.
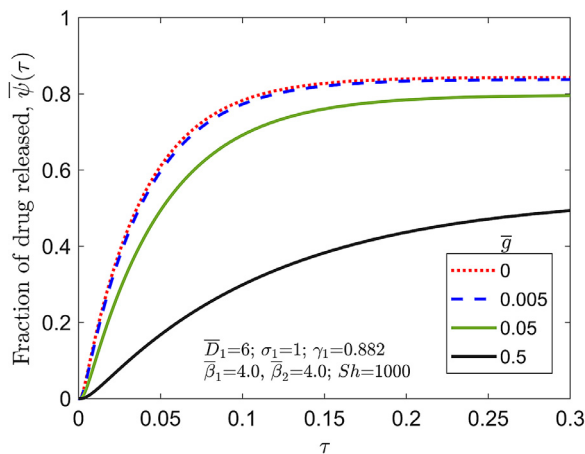

Fig. 11. Effect of thin outer coating: $\bar{\psi}(\tau)$ as a function of τ for multiple values of $\bar{l}$. Other problem parameters are $\bar{D}_1 = 6$; $\sigma_1 = 1$; $\gamma_1 = 0.882$; $\bar{\beta}_1 = \bar{\beta}_2 = 4$; $Sh = 1000$.

a longer time, which reduces the total mass of drug that is eventually released. Fig. 10 shows rapid release of the drug starting at $\tau = 0$ for a thin shell. As the shell becomes thicker and thicker, the curve becomes flatter and flatter at early times, due to the finite time taken for diffusion through the shell. Fig. 10 shows that while a thick shell may result in more steady drug release over a longer time, which may be desirable for some conditions, however, having a thick shell may also necessitate greater initial loading due to the increased propensity of absorption.

Fig. 11 presents the impact of the thickness and diffusion coefficient of the coating on drug release characteristics. The fraction of drug released is plotted as a function of time for multiple values of the non-dimensional coating parameter $\bar{g}$, including the baseline curve for no coating, $\bar{g} = 0$. Fig. 11 shows negligible impact of the coating on the drug release characteristics when $\bar{g}$ is small. However, as $\bar{g}$ rises, the drug release curve slows down due to the resistance offered by the coating. In addition, due to the absorption processes that occur within the core and shell, this also results in reduced mass of drug released. Similar to the impact of Sh, this means a more gradual release when $\bar{g}$ is large, but the trade-off is the reduction in the total mass of drug released. Note that the resistance-based model described above is likely to lose accuracy as the coating becomes thicker and thicker because this model inherently neglects the transient concentration gradients within the coating.

6. Conclusions

Experimental investigation of drug release from capsules typically involves multiple experiments involving several different design configurations. The time and costs associated with these experiments is often excessive. The mathematical model and analysis presented here may potentially help in early stage evaluation and down-selection of candidate drug delivery materials and geometries. While some existing literature is available on a two-layer capsule for specific applications, the present work generalizes this treatment by presenting a solution for an arbitrary number of layers that accounts for binding reactions within the capsule, as well as general convective boundary conditions on the outside, therefore accounting for multiple types of micro-environment around the capsule. Despite some simplifying assumptions, the model presented here is able to provide a closed-form solution for drug diffusion dynamics through a multi-layer capsule. In addition to providing theoretical insights into the fundamental nature of this problem, the analytical solution is also expected to offer reduced computational cost compared to a full-scale numerical calculation.

It is important to recognize key assumptions and limitations of the present one-dimensional model. Binding reactions within the sphere are modeled using first-order reaction kinetics. Drug dynamics in the medium outside the capsule are ignored, so that the interactions between the capsule and the medium are represented entirely by the boundary condition. Diffusion coefficients are assumed to be independent of concentration. For most practical applications, such assumptions may be reasonable, and therefore, model results may be helpful in evaluation of materials/geometries and design of experiments.

Declaration of Competing Interest

All authors hereby declare that they do not have conflicts of interest as described by Elsevier's policies (http://www.elsevier.com/conflictsofinterest).

Acknowledgements

Appendix A. Derivation of the eigenequation and expressions for coefficients $A_{m,n}$ and $B_{m,n}$

A formal derivation of the eigenequation for the general M-layer case is presented below. In short, several coefficients appearing in Eqs. (16)–(19) are systematically eliminated, and finally, the ratio of the coefficients for the Mth layer is written in two different ways, leading to the eigenequation.

To begin with, one may write $A_{m,n}$ in terms of $B_{m,n}$, and $B_{m,n}$ in terms of $B_{1,n}$ as follows:

$$\eta_{m,n}(\lambda_n) = \frac{A_{m,n}}{B_{m,n}} \tag{A.1}$$

$$B_{m,n} = B_{1,n}\Phi_m \tag{A.2}$$

so that, from Eq. (14), one may write

$$f_{m,n}(\xi) = B_{1,n}\Phi_m q_{m,n}(\xi) \tag{A.3}$$

where

$$\Phi_1 = 1 \tag{A.4}$$

$$\Phi_m = \frac{\sigma_{m-1}q_{m-1,n}(\gamma_{m-1})}{q_{m,n}(\gamma_{m-1})} \cdot \frac{\sigma_{m-2}q_{m-2,n}(\gamma_{m-2})}{q_{m-1,n}(\gamma_{m-2})}$$
$$\cdots \frac{\sigma_2 q_{2,n}(\gamma_2)}{q_{3,n}(\gamma_2)} \cdot \frac{\sigma_1 q_{1,n}(\gamma_1)}{q_{2,n}(\gamma_1)} \quad (m = 2,3\ldots M) \tag{A.5}$$

with

$$q_{m,n}(\xi) = \eta_{m,n}(\lambda_n)\frac{\cos(\omega_{m,n}\xi)}{\xi} + \frac{\sin(\omega_{m,n}\xi)}{\xi} \tag{A.6}$$

Further, from Eqs. (16) and (17), the functions $\eta_{1,n}(\lambda_n)$ and $\eta_{M,n}(\lambda_n)$ are given by

$$\eta_{1,n}(\lambda_n) = 0 \tag{A.7}$$

$$\eta_{M,n}(\lambda_n) = -\frac{1 - \omega_{M,n}\cot(\omega_{M,n}) - Sh}{\cot(\omega_{M,n}) + \omega_{M,n} - Sh \cdot \cot(\omega_{M,n})} \tag{A.8}$$

Now, by using Eq. (13) in Eq. (11), and using equations (A.3) and (A.5), one may write

$$\bar{D}_m \dot{q}_{m,n}(\gamma_m) = \frac{\bar{D}_{m+1}\sigma_m q_{m,n}(\gamma_m)\eta_{m+1,n}(\lambda_n)\left[\frac{-\omega_{m+1,n}\sin(\omega_{m+1,n}\gamma_m)\gamma_m - \cos(\omega_{m+1,n}\gamma_m)}{\gamma_m^2}\right]}{\eta_{m+1,n}(\lambda_n)\frac{\cos(\omega_{m+1,n}\gamma_m)}{\gamma_m} + \frac{\sin(\omega_{m+1,n}\gamma_m)}{\gamma_m}}$$
$$+ \frac{\bar{D}_{m+1}\sigma_m q_{m,n}(\gamma_m)\left[\frac{\omega_{m+1,n}\cos(\omega_{m+1,n}\gamma_m)\gamma_m - \sin(\omega_{m+1,n}\gamma_m)}{\gamma_m^2}\right]}{\eta_{m+1,n}(\lambda_n)\frac{\cos(\omega_{m+1,n}\gamma_m)}{\gamma_m} + \frac{\sin(\omega_{m+1,n}\gamma_m)}{\gamma_m}} \tag{A.9}$$

which, with some simplification, results in

$$\eta_{m+1,n}(\lambda_n)$$
$$= \frac{\bar{D}_{m+1}\sigma_m q_{m,n}(\gamma_m)[\omega_{m+1,n}\cot(\omega_{m+1,n}\gamma_m)\gamma_m - 1] - \bar{D}_m\dot{q}_{m,n}(\gamma_m)\gamma_m}{\bar{D}_{m+1}\sigma_m q_{m,n}(\gamma_m)[\omega_{m+1,n}\gamma_m + \cot(\omega_{m+1,n}\gamma_m)] + \bar{D}_m\dot{q}_{m,n}(\gamma_m)\cot(\omega_{m+1,n}\gamma_m)\gamma_m} \tag{A.10}$$

Note that the over-dot denotes the derivative with respect to ξ_m.

Equation (A.10) is valid at each interface, $m = 1,2,3..M$-1. Setting $m = M$-1 in Eq. (A.10) and comparing with Eq. (A.8) results in elimination of the coefficients and therefore, an equation that governs the eigenvalues λ_n. Therefore, the eigenequation for the general M-layer problem is:

$$\frac{\bar{D}_M\sigma_{M-1}q_{M-1,n}(\gamma_{M-1})[\omega_{M,n}\cot(\omega_{M,n}\gamma_{M-1})\gamma_{M-1} - 1] - \bar{D}_{M-1}\dot{q}_{M-1,n}(\gamma_{M-1})\gamma_{M-1}}{\bar{D}_M\sigma_{M-1}q_{M-1,n}(\gamma_{M-1})[\omega_{M,n}\gamma_{M-1} + \cot(\omega_{M,n}\gamma_{M-1})] + \bar{D}_{M-1}\dot{q}_{M-1,n}(\gamma_{M-1})\cot(\omega_{M,n}\gamma_{M-1})\gamma_{M-1}}$$
$$+ \frac{1 - \omega_{M,n}\cot(\omega_{M,n}) - Sh}{\cot(\omega_{M,n}) + \omega_{M,n} - Sh \cdot \cot(\omega_{M,n})} = 0 \tag{A.11}$$

Once the eigenvalues are determined from the roots of the transcendental equation (A.11), the coefficients $A_{m,n}$ and $B_{m,n}$ may be determined by assuming one of the coefficients, say, $B_{1,n}$ to be one, and determining all other coefficients in terms of $B_{1,n}$ from Eqs. (16)-(19). This is possible because Eqs. (16)-(19) are homogeneous, and, therefore, an infinite number of solutions exist, provided that the determinant of the equations is zero, which is equivalent to equation (A.11) being satisfied.

From Eq. (16), $A_{1,n} = 0$. An iterative expression for determining $A_{m+1,n}$ and $B_{m+1,n}$ in terms of $A_{m,n}$ and $B_{m,n}$ for each $m = 1,2,3..M$-1 is derived here.

From Eq. (18)-(19), the following pair of linear algebraic equations may be written for $A_{m+1,n}$ and $B_{m+1,n}$ for each $m = 1,2,3..M$-1

$$a_{m,n}A_{m+1,n} + b_{m,n}B_{m+1,n} = u_{m,n} \tag{A.12}$$

$$d_{m,n}A_{m+1,n} + e_{m,n}B_{m+1,n} = v_{m,n} \tag{A.13}$$

where

$$a_{m,n} = \cos(\omega_{m+1,n}\gamma_m); \; b_{m,n} = \sin(\omega_{m+1,n}\gamma_m); \; d_{m,n} = -\bar{D}_{m+1}$$
$$[\cos(\omega_{m+1,n}\gamma_m) + \omega_{m+1,n}\gamma_m\sin(\omega_{m+1,n}\gamma_m)];$$
$$e_{m,n} = -\bar{D}_{m+1}[\sin(\omega_{m+1,n}\gamma_m) - \omega_{m+1,n}\gamma_m\cos(\omega_{m+1,n}\gamma_m)] \tag{A.14}$$

$$u_{m,n} = \sigma_m[A_{m,n}\cos(\omega_{m,n}\gamma_m) + B_{m,n}\sin(\omega_{m,n}\gamma_m)] \tag{A.15}$$

$$v_{m,n} = \bar{D}_m[-A_{m,n}\cos(\omega_{m,n}\gamma_m) - B_{m,n}\sin(\omega_{m,n}\gamma_m)$$
$$+ \omega_{m,n}\gamma_m[-A_{m,n}\sin(\omega_{m,n}\gamma_m) + B_{m,n}\cos(\omega_{m,n}\gamma_m)]] \tag{A.16}$$

Eqs. (A.12)-(A.13) represent a set of two linear equations in $A_{m+1,n}$ and $B_{m+1,n}$, which may be solved easily to result in

$$A_{m+1,n} = \frac{e_{m,n}u_{m,n} - b_{m,n}v_{m,n}}{a_{m,n}e_{m,n} - b_{m,n}d_{m,n}}; \; B_{m+1,n} = \frac{-d_{m,n}u_{m,n} + a_{m,n}v_{m,n}}{a_{m,n}e_{m,n} - b_{m,n}d_{m,n}} \tag{A.17}$$

Note that $u_{m,n}$ and $v_{m,n}$ are known in terms of $A_{m,n}$ and $B_{m,n}$. Therefore, $A_{m+1,n}$ and $B_{m+1,n}$ may be recursively determined in terms of $A_{m,n}$ and $B_{m,n}$ for $m = 1,2..M$-1 using Eqs. (A.17).

References

[1] D.Y. Arifin, L.Y. Lee, C.H. Wang, Mathematical modeling and simulation of drug release from microspheres: implications to drug delivery systems, Adv. Drug Deliv. Rev. 58 (2006) 1274–1325.

[2] A.S. Timin, D.J. Gould, G.B. Sukhorukov, Multi-layer microcapsules: fresh insights and new applications, Expert Opin. Drug. Deliv. 14 (2016) 583–587.

[3] A. Larrañaga, M. Lomora, J.R. Sarasua, C.G. Palivan, A. Pandit, Polymer capsules as micro-/nanoreactors for therapeutic applications: current strategies to control membrane permeability, Prog. Mater. Sci. 90 (2017) 325–357.

[4] S. De Koker, R. Hoogenboom, B.G. De Geest, Polymeric multilayer capsules for drug delivery, Chem. Soc. Rev. 41 (2012) 2867–2884.

[5] J. Majumder, T. Minko, Multifunctional and stimuli-responsive nanocarriers for targeted therapeutic delivery, Exp. Opin. Drug Deliv. 18 (2021) 205–227.

[6] A. Hadjitheodorou, G. Kalosakas, Analytical and numerical study of diffusion–controlled drug release from composite spherical matrices, Mater. Sci. Eng. C 42 (2014) 681–690.

[7] J. Siepmann, F. Siepmann, Mathematical modelling of drug dissolution,' Int. J. Pharmaceutics 453 (2013) 12–24.

[8] G. Pontrelli, G. Toniolo, S. McGinty, D. Peri, S. Succi, C. Chatgilialoglu, Mathematical modelling of drug delivery from pH-responsive nanocontainers, Comput. Biol. Med. 131 (2021) 104238.

[9] A. Jain, M. Parhizi, L. Zhou, G. Krishnan, Imaginary eigenvalues in multilayer one-dimensional thermal conduction problem with linear temperature-dependent heat generation,' Int. J. Heat Mass Transfer 170 (2021) pp. 120993:1-10.

[10] J. Pérez, C. Picioreanu, M. van Loosdrecht, Modeling biofilm and floc diffusion processes based on analytical solution of reaction-diffusion equations, Water Res. 39 (2005) 1311–1323.

[11] H. Wilhelmsson, E. Lazzaro, Reaction-Diffusion Problems in the Physics of Hot Plasmas, CRC Press, Boca Raton, 2000 ISBN: 9781420033588.

[12] E.B. Nauman, Chemical Reaction Design, Optimization and Scaleup, 2nd Ed., John, Wiley & Sons, Hoboken, NJ, 2008 ISBN: 9780470282069.

[13] N.F. Britton, Reaction-Diffusion Equations and Their Applications to Biology, 1st Ed., Academic Press, Orlando, FL, 1986 ISBN: 9780121351403.

[14] J. Siepmann, F. Siepmann, Modeling of diffusion controlled drug delivery, J. Control. Release 161 (2012) 351–362.

[15] J. Siepmann, R.A. Siegel, M.J. Rathbone, Fundamentals and Applications of Controlled Release Drug Delivery, Springer, 2012.

[16] P.L. Ritger, N.A. Peppas, A simple equation for description of solute release I. Fickian and non-fickian release from non-swellable devices in the form of slabs, spheres, cylinders or discs, J. Control. Release 5 (1987) 23–36.

[17] J. Siepmann, F. Siepmann, Mathematical modelling of drug delivery,', Int. J. Pharmaceutics 364 (2008) 328–343.

[18] S. McGinty, A decade of modelling drug release from arterial stents, Mathematical Biosci. 257 (2014) 80–90.

[19] S. Fredenberg, M. Reslow, A. Axelsson, The mechanisms of drug release in poly(lactic-co-glycolic acid)-based drug delivery systems–a review, Int. J. Pharmaceutics 415 (2011) 34–52.

[20] G. Pontrelli, F. de Monte, Modeling of Mass Dynamics in Arterial Drug-Eluting Stents, J. Porous Media 12 (2009) 19–28.

[21] E.J. Carr, G. Pontrelli, Modelling mass diffusion for a multi-layer sphere immersed in a semi-infinite medium: application to drug delivery, Mathematical Biosci. 303 (2018) 1–9.

[22] B. Kaoui, M. Lauricella, G. Pontrelli, Mechanistic modelling of drug release from multi-layer capsules, Comput. Biol. Med. 93 (2018) 149–157.

[23] S. McGinty, D. King, G. Pontrelli, Mathematical modelling of variable porosity coatings for controlled drug release, Medical Eng. Phys. 45 (2017) 51–60.

[24] M. Vynnycky, S. McKee, M. Meere, C. McCormick, S. McGinty, Asymptotic analysis of drug dissolution in two layers having widely differing diffusivities, IMA J. Appl. Math. 84 (2019) 533–554.

[25] M. Mikhailov, M. Özişik, Unified Analysis and Solutions of Heat and Mass Diffusion, Dover Publications, New York, 1994.

[26] D. Hahn, M. Özişik, Heat Conduction, Wiley, New York, 2012.

[27] K. Gudnason, S. Sigurdsson, B. Snorradottir, M. Masson, F. Jonsdottir, A numerical framework for drug transport in a multi-layer system with discontinuous interlayer condition, Mathematical Biosci. 295 (2018) 11–23.

[28] T. Köddermann, D. Reith, A. Arnold, Why the Partition Coefficient of Ionic Liquids Is Concentration-Dependent,', J. Phys. Chem. B 117 (2013) 10711–10718.

[29] A. Tzafriri, A. Levin, E. Edelman, Diffusion-limited binding explains binary dose response for local arterial and tumour drug delivery, Cell Prolif. 42 (2009) 348–363.

[30] S. Henning, D. Edelhoff, B. Ernst, S. Leick, H. Rehage, D. Suter, Characterizing permeability and stability of microcapsules for controlled drug delivery by dynamic NMR microscopy, J. Magn. Reson. 221 (2012) 11–18.